Journal of Nanoscience and Nanotechnology
Vol. 12, 5552–5557, 2012

RESEARCH ARTICLE

Ohmic Contact Effect of Ag-Nanodots on Quantum Efficiency of Si Solar Cell

Jaeho Choi, Bhaskar Parida, Hyung Yong Ji, Seungil Park, and Keunjoo Kim*

Department of Mechanical Engineering and Research Center of Industrial Technology, Chonbuk National University, Jeonju 561-756, R. O. Korea

The authors investigated Si solar cell with the inclusion of nano-Ag dots using the ink-jet printer. These nano-Ag dots were used for the Ohmic contact layer on phospho-silicate glass layer, which was not removed after the formation of Si emitter layer by phosphorus diffusion process. The SiN_x layer deposited on the nano-Ag dots shows the catalyst selective growth and so the layer formed beneath of nano-Ag dots. The photoreflectances show that the long wavelength from 360 nm to 1200 nm tends to be increased as the density of the nano-Ag is increased. In case of short wavelength from 294 nm to 367 nm, it shows the opposite trend, indicating the plasmon effect of the nano-Ag. As embedding the nano-Ag dots on the phospho-silicate glass layer, the blocked Ohmic contact was opened and the quantum efficiency of 14.4% was achieved, which is higher than the reference sample of 12.72% without the glass layer. The nano-Ag dots form the good Ohmic contact and also enhance the light conversion efficiency with the formation of surface plasmon.

Keywords: Silicon Solar Cell, Nano-Ag Dots, Quantum Efficiency, Surface Plasmon.

1. INTRODUCTION

Si solar cell has been extensively investigated in order to improve the cell efficiency by introducing nanostructures such as semiconductor quantum dots, photonic crystals, nanoporous Si, and metallic nanoparticles.[1–4] Metallic nanoparticles such as Cu, Au, Al, and Ag can be used in Si solar cells to increase the device efficiency by increasing the light absorption.[5–7] Ag nanoparticles are widely used in solar cells for their light scattering nature at proper particle size[8–9] and strong enhancement of electric field at the visible and near infrared region of light that occurs due to the localized surface plasmon. This localized surface plasmon enhances the light absorption into the solar cell and increases the photocurrent.[10, 11] Furthermore, a 16-fold increase in photocurrent has been achieved for a 1.25 μm silicon-on insulator cells by using Ag nanoparticles in which light is coupled into the optically dense over a broad angular range when the localized surface plasmon resonance in the Ag nanoparticles are excited by the incident light.[6]

In conventional solar cell fabrication process,[12–14] the phospho-silicate glass (PSG) which is a dielectric layer formed during the phosphorus duffision, is removed due to its low absorption coefficient of light at long wavelengths. But this dielectic layer associated with metallic nanoparticles like Ag nanoparticles develops a tunable light trapping for solar cells. Ag nanoparticles with dielectric layer markedly enhances the redshift and tuned the localized surface plasmon resonance to longer wavelengths to be coupled into the cell for photocurrent enhancement.[15, 16] The silicate glass layer is used in the high efficiency crystalline solar cells for the front surface passivation and backside thick oxide under the contacts that supressess the recombination and increase the internal reflection. Furthermore, the PSG layer is used as a dopant source to form selective emitter by laser doping process in which the laser selectively melts the silicon and drives the phosphorus in the emitter deep into the wafer and reduces the sheet resistance underneath the contact finger to achieve high internal quantum efficiency.[17] Therefore, it is valuable to clarify the plasmon effect of Ag nanoparticles to enhance the reduction of contact resistance from the interaction with the dielectric PSG layer on the surface of Si solar cells.

In this work, we investigated polycrystalline Si solar cell with the inclusion of nano-Ag dots. We printed Ag nanoparticles on the silicon solar cell wafers without removing PSG layer by ink-jet printer, where the nano-Ag dots arrays were placed between PSG layer and SiN_x, antireflection coating, and was compared with the reference samples with and without PSG layers. Nano-Ag dots on PSG layer enhance the conversion efficiency of 1.65%

*Author to whom correspondence should be addressed.

1533-4880/2012/12/5552/006 doi:10.1166/jnn.2012.6400

to compare to the reference sample without PSG layer and also provide the plasmonic conduction channel to compare to the reference sample with PSG layer.

2. EXPERIMENTAL DETAILS

Si solar cell was fabricated with the inclusion of nano-Ag dots using ink-jet printer instead of any other deposition or spray process because of its low cost and simplicity[18] to maintain uniformity of the Ag nano-dot on the cell. The schematic diagram is shown in Figure 1. A p-type 6-in polycrystalline Si solar cell wafer with the average sheet resistance of 47 Ω/sq was used. In order to increase the absorption of light, the wafer surface was textured. In typical texturing process, polycrystalline Si solar cell is usually textured by using acid solution. The isotropic etching with the mixture solution of HF:HNO_3: CH_3COOH was carried out and the oxidized surface was etched by HF solution. The p-n junction was formed on the textured wafer by using a tube furnace with $POCl_3$ as the dopant source. In tube furnace, the process of phosphorus diffusion has two steps, such as pre-deposition process and drive-in process. Pre-deposition process is carried out at 820 °C for 7 min and makes the phosphorus concentration uniform on solar cell surface. The drive-in process diffuses dopants in solar cell at the temperature of 860 °C for 16 min. The sheet resistance was 49.6 Ω/sq, measured by the 4 points probe method and the lifetime was 13.9 μs. In drive-in process, the PSG layer was formed on solar cell surface due to the SiO_2:P_2O_5 reaction. The PSG layer is usually removed in the standard solar cell process. But in this work, we did not remove the PSG layer in order to understand the Ohmic contact effect of nano-Ag dots which were ink-jet printed on the solar cell. The nano-Ag dots have the size distribution of 10~50 nm.

After ink-jet printing of nano-Ag dots arrays on PSG layer, a 80 nm thickness of SiN_x as the anti-reflection coating was deposited in the ambient gas mixture of SiH_4 and NH_3 by using plasma enhanced chemical vapor deposition (PECVD). The bus and finger metal contacts were printed by screen printing of Ag paste. The back metallization was carried out by screen printing technique using Al paste. Then the drying process was carried out at 270 °C for 60 sec, and co-fired at 790 °C for 90 sec in a belt-type furnace. Finally the laser edge isolation was proceessed to improve the parallel resistance. The nano-Ag dots sample with PSG layer was compared to the two reference (Ref.) samples with and without PSG layers. Furthermore, the nano-Ag dots sample was partitioned to 4 quadrants in the printing process of Ag nanoparticles.

Figure 2 shows the photographic image of the fabricated 6-in solar cell which shows the light blue surface due to the PSG layer as compared to the nomal standard solar cell. The nano-Ag dots were printed on 4 equal parts of the solar cell. The second quadrant was selected as the Ref. without any Ag dots on the PSG layer, and other quadrants were nano-Ag dot printed with the line intervals of 160, 120, and 80 μm with the line width of 40 μm on the first, third and fourth quadrants respectively. The sample parts were named as Ref., Ag160, Ag120 and Ag80.

3. RESULTS AND DISCUSSION

Figure 3 shows the top and cross-sectional FE-SEM images of the ink-jet printed nano-Ag dots on the fabricated solar cell. Figure 3(a) shows the nano-Ag pattern ink-jet printed on solar cell surface and Figures 3(b), (c) and (d) are the magnified images where we can see that most nano-Ag dots are located as well as aggregated at the sunken parts of the textured wafer surface. The aggregation of the nano-Ag dots is formed due to the dry and co-firing process. The Figures 3(e) and (f) are the cross-sectional images of the solar cell where the nano-Ag of dots are found above the SiN_x layer which is a contrast. Even though the SiN_x layer was deposited on the nano-Ag dots, nano-Ag dots were located on the surface of solar

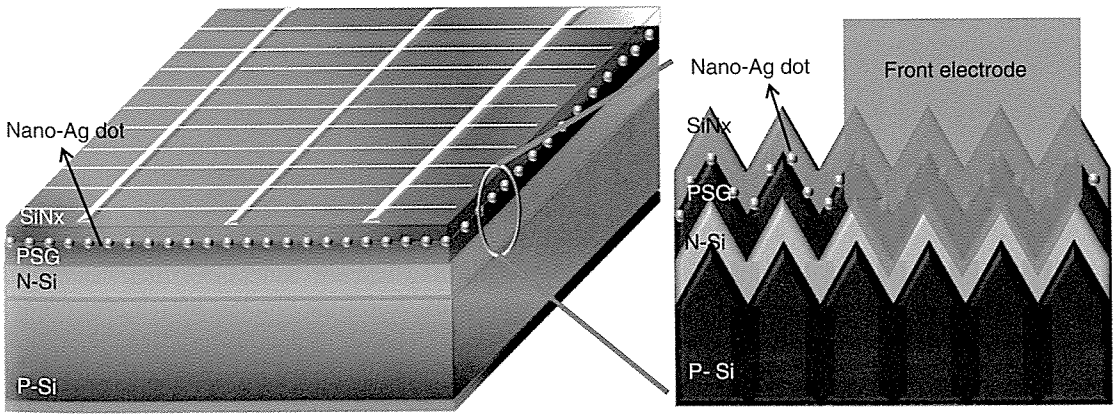

Fig. 1. Schematic diagram of the Si solar cell structure with the inclusion of nano-Ag dots. The nano-Ag dots were printed by non-contact ink-jet printer and the PSG layer remained on the emitter surface in the standard fabrication process of Si solar cells. The nano-Ag dots with the size of 10~50 nm were printed on the PSG later.

RESEARCH ARTICLE

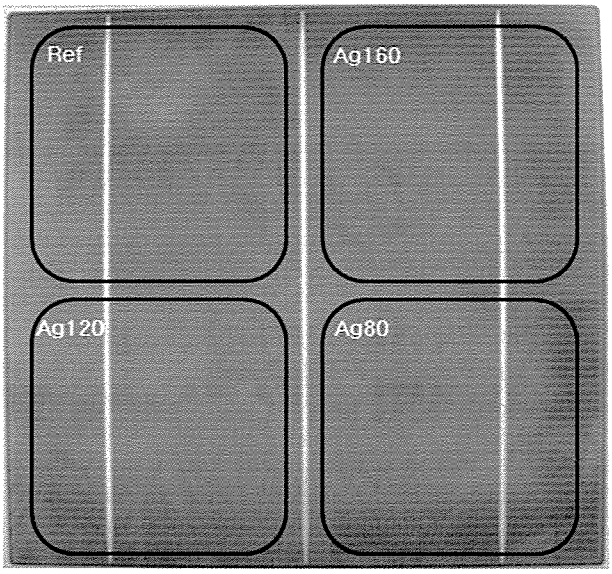

Fig. 2. Photograph of 6-in Si solar cell which was processed with the inclusion of nano-Ag dots on PSG layer. The color of the sample surface with the PSG layer shows a lightly blue rather than the dark blue for the standard cell without PSG layer. We prepared samples with the different densities of the nano-Ag dots. The 40-μm width ink lines including nano-Ag dots were printed with the line intervals of 80, 120, and 160 μm.

cell as shown in FE-SEM images. This indicates that SiN_x layer can be selectively grown up due to the catalystic effect of nano-Ag dots. For the case of the part without the nano-Ag dots, no selective growth of SiN_x was found.

Furthermore, the nano-Ag dots can react with the SiN_x precursors in PECVD process. The nano-Ag particles

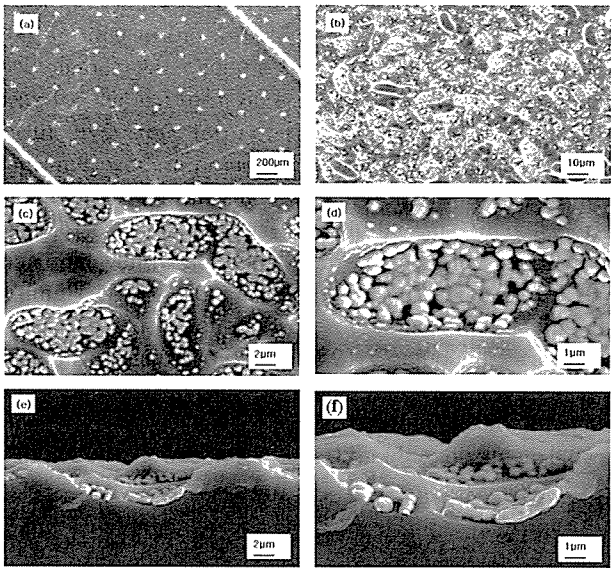

Fig. 3. FE-SEM images on the surface of Si solar cell including nano-Ag dots. The image (a) shows the micro-ink dots printed by inkjet using nano-Ag ink and the farther images show the magnified views on the nano-Ag dots. The 80-nm thick SiN_x layer deposited on the nano-Ag dots layer could not cover the nanoparticles due to the catalystic selective growth.

surrounded by the SiN_x thin film coats the particles, so that the size of Ag nanoparticles is about 300~600 nm as shown in Figure 3(f). The Ag films with few nanometer thickness deposited by e-beam evaporation on the SiN_x film grown by PECVD can form the nanoparticles by the thermal treatment at the temperature of 700 °C.[19] The Ag-SiN_x interface provides the good environment of the selective growth of semiconductor materials such as Si and ZnO.[20] Similarly, the SiN_x thin film deposition on the nano-Ag dots placed on Si surface provides the selective growth condition. The plasma supplies the energy for the charge oscillations of electrons at the surfaces of nano-Ag dots, so that the surface charge polarization induces the coating of SiN_x thin film. The coated nano-Ag dots can form the modified internal electromagnetic field expressed to $E_i = 3E_0(\varepsilon_d/(\varepsilon_m + 2\varepsilon_d))$, where E_0 is the Ref. internal field and ε_d and ε_m are the permittivities of the SiN_x and Ag, respectively.[21] The enhancement of the internal electric field near the nano-Ag dots can influence on the light absorption.

The photographic images of PL and EL about cell are presented in Figure 4. Overall, both PL and EL images of all parts show the well-matched dark spots and the contrast of PL is better than that of EL with the magnification gain of 31 under the measurement conditions of the bias of 0.9 V and the current of 0.5 A with camera exposure time of 1.5 sec. The high PL spectra indicate that the *p–n* junction formation is well-defined. Generally, the dark parts of the PL show low shunt resistance related to the *p–n* junction and the dark parts of EL show high series resistance of shunt resistance. In case of Ref. quadrant the PL is relatively darker than other quadrants. This seems to be related to the enhanced light emission for the samples with the inclusion of nano-Ag dots on the PSG layer. In case of Ag80, both PL and EL images seem to be dark with low shunt resistance. The problem of the low shunt resistance reduces the current and voltage flow due to the leakage current across the p-n junction in the solar cell and this means that the nano-Ag reduces series resistance in PSG layer, so that the Ohmic contact gets better.

In the standard Si p-n junction solar cell, PL and EL emissions are very sensitve on the series and shunt resistances. The dark solar cell region for both PL and EL images has the very low shunt resistance in p-n junction, which causes the carrier recombination process due to the formation of defect levels in the depletion region. The optically or electrically pumped electrons could not be back to valence band indicating that the high shunt resistance shows the similar emission effect for both PL and EL. However, the series resistance does not. The solar cell region with bright PL and dark EL images has too high series resistance. The good conditions of solar cell are for both bright PL and EL images with high shunt and low series resistances. Therefore, the dark regions in both PL and EL images have the unstable doping behavior

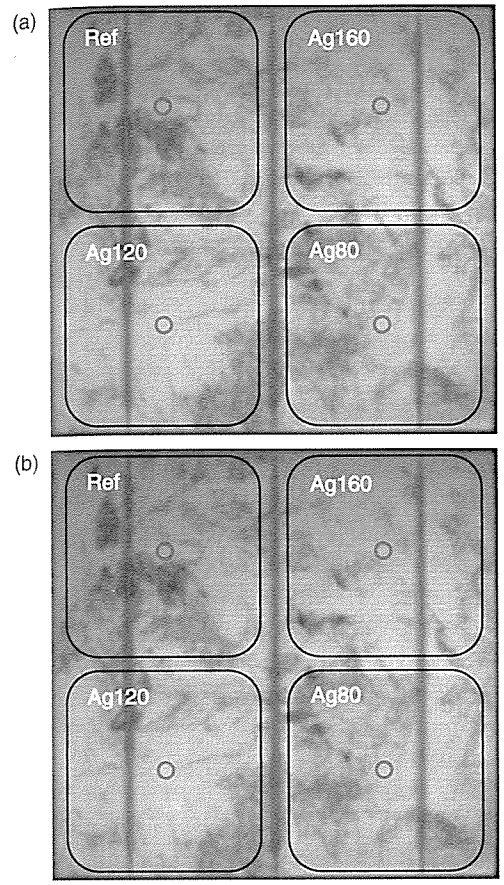

Fig. 4. Light emission images of (a) PL and (b) EL with the magnification gain of 31 from the 6-in wafer Si solar cell. The circled areas are the probing positions on the quantum efficiency. The bright areas in both PL and EL spectra have the relatively high shunt resistance because the luminescence signal is related to the local junction voltage. The dark areas in both PL and EL spectra have the relatively low shunt resistance and the different contrast area has the relatively high series resistance.

for the polycrystalline Si grains with various crystalline planes such as (110) where the doping channeling effect can occur.

Figure 5 shows the photoreflectance spectra of Si solar cell with the inclusion of printed nano-Ag dots. The Ref. sample shows low photoreflectance in the nearly visible wavelength of 367 nm and high photoreflectance in the UV region at wavelength of 228 nm as compared to the Ag160, Ag120 and Ag80. Furthermore, the Ref. shows absorption of light in the wavelength of 304 nm and also at the wavelength of 1012 nm. The photoreflectances of Ag160, Ag120 and Ag80 are same at the nearly visible light at the wavelength of 376 nm where as the Ag80 shows the lowest photoreflectance in the UV region at the wavelength of 228 nm, high photo-absorption at the wavelength of 313 nm and little high photoreflectance in the infrared region as compared to the Ag160 and Ag120. This implies that, as the densities of nano-Ag dots are increased, photoreflectances are decreased in the UV region and the photo-absorptions are increased from 304 nm to 313 nm,

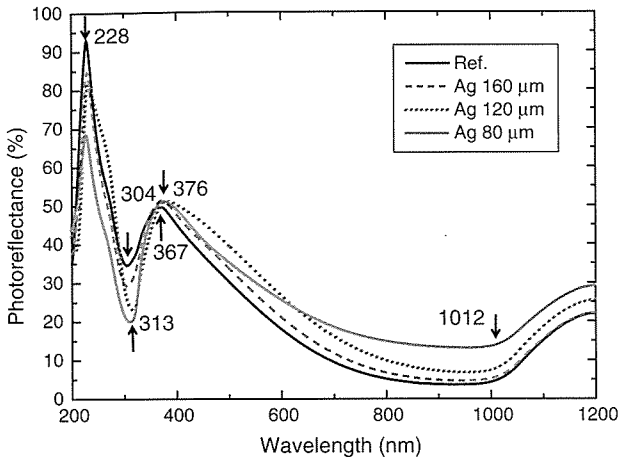

Fig. 5. Photoreflectances of Si solar cell with the inclusion of nano-Ag dots. As the densities of nano-Ag dots are increased, photoreflectances are increased to compare to the Ref. sample in the larger spectral region of the wavelength than 367 nm. However, for the wavelength region below 367 nm, the photoreflectances are proportional, indicating the contribution of the plasmon effect of nano-Ag dots.

but as compared to the Ref. sample the photoreflectance increases in the nearly visible region of wavelength from 367 nm to 376 nm. The photoreflectance below the region of wavelength of 367 nm are decreased which indicates the contribution of the plasmon effect of nano-Ag dots.

According to the Mie theory for a nanoparticle, the size-dependent contribution on the plasmonic effect is very sensitive on optical absorption.[22] The absorption of solar light can be enhanced by the excitation of surface plasmons of metal nanoparticles with the optimal diameter of about $d = 50$ nm. Furthermore, the extinction cross-section $\sigma(\lambda)$ in the long wave length limit can be written as[23]

$$\sigma(\lambda) = \frac{3\pi^2 d^3 \epsilon_d^{3/2}}{\lambda}\left[\frac{\epsilon_{im}}{(\epsilon_{rm}+2\epsilon_d)^2+\epsilon_{im}^2}\right]$$

where d is the diameter of the metallic nanospheres, ϵ_d is the dielectric constant of the medium surrounding the nanosphere, λ is the wavelength, ϵ_{rm} and ϵ_{im} are the real and imaginary parts of the metal dielectric function. This formula predicts a surface plasmon resonant peak when $\epsilon_{rm} = -2\epsilon_d$ which for Ag occurs in the UV portion of the spectrum. The surface plasmon resonance frequency is $\omega_R = \omega_p/[\epsilon_{rm}^b(\omega_R) + 2\epsilon_d]^{1/2}$ and $\omega_p = (ne^2/m\epsilon_0)^{1/2}$, where ω_p is the plasma frequency and ϵ_{rm}^b is the metal dielectric function of the interband transition, respectively. When the dielectric constant of the medium is changed, the peak position of resonance wavelength is shifted. Therefore, the enhanced photo-absorption below the wavelength of 367 nm comes from the dominant plasmonic effect of light absorption and the enhanced photoreflectance above the wavelength of 367 nm, comes from the dominant plasmonic effect of light scattering on nanoparticles.

Figure 6 shows quantum efficiencies of Si solar cell with the inclusion of nano-Ag dots. In case of Ref. sample,

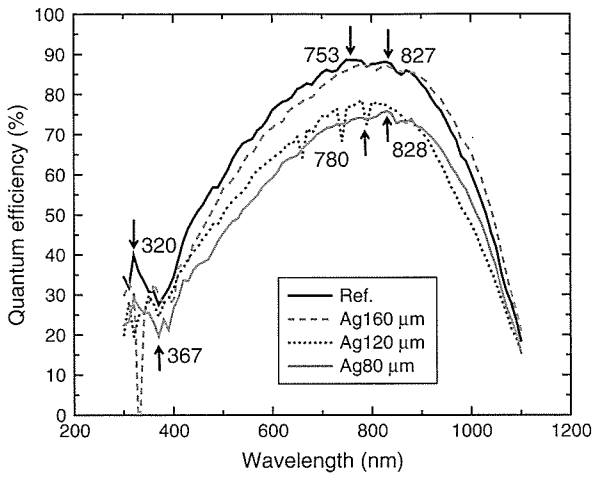

Fig. 6. Quantum efficiencies of Si solar cell with the inclusion of nano-Ag dots. As the densities of nano-Ag dots are increased, the efficiencies are decreased.

quantum efficiency shows the highest value in the spectral range below 827 nm and the efficiency decreases with the increasing density of nano-Ag dots. However, for the spectral range above 827 nm, the sample of Ag120 shows the lower efficiency than the sample of Ag80 above the wavelength of 828 nm. The Ref. sample shows the highest peak position at the wavelength of 753 nm. For the samples of Ag160, Ag120, and Ag80, the peak positions are located at the wavelengths of 827, 780, and 828 nm, respectively. The quantum efficiency is inversely proportional to the photoreflectance. The nano-Ag dot arrays result in the reduced quantum efficiency with the increased photoreflectance in the overall spectral range. The high density spacing of the nano-Ag dots by ink-jet printing technique blocks the light absorption, so that the quantum efficiency is limited.

The surface-coated nano-Ag dots with SiN_x layer produce strong scattering of light at a particular wavelength due to the localized surface plasmons. This effect causes the modification of the photoreflectance and the light trapping. For the nano-Ag dots with the size of 200 nm, the quantum efficiency is improved in the spectral range between 600 and 800 nm with the corresponding absorption enhancement above the wavelength of 600 nm.[24] However, all samples with nano-Ag dots show the decreased efficiency for the spectral range between 368 and 827 nm. Even though the sample of Ag120 shows the higher photoreflectance than the Ref. sample without nano-Ag dots, it shows the enhanced efficiency above the spectral range of 827 nm.

Table I shows the cell efficiency of reference samples and Ag nanodots printed solar cell measured under a simulated AM 1.5 sun spectrum. The efficiency of reference sample with PSG layer was about 0.994% with open circuit voltage (V_{oc}) of 0.0028 V, the short circuit current (I_{sc}) of 0.464 A, and fill factor (FF) of 1.07 with the series resistance (R_s) of 0.00029 Ω and the shunt resistance (R_{sh})

Table I. Efficiency data of the Ref. and nano-Ag printed solar cell by measured solar simulator under the condition of AM 1.5 illuminations. The efficiency of Ref. solar cell with PSG layer was measured to be 0.994% and it was increased to 12.72% for the Ref. sample without PSG layer. Furthermore, the efficiency of nano-Ag printed solar cell was measured to be 14.37%.

	V_{oc}	I_{sc}	FF	N_{cell}	R_s	R_{sh}
Ref. with PSG	0.0028	0.4645	1.0704	0.994	0.00029	4.6687
Ref. w/o PSG	0.5910	6.919	75.71	12.721	0.00070	6.644
Nano-Ag	0.605	7.69	77.118	14.375	0.00295	13.427

of 4.668 Ω. However, the efficiency of reference sample without PSG layer was about 12.72% with $V_{oc} = 0.591$ V, $I_{sc} = 6.919$ A and FF = 75.71 with $R_s = 0.00070$ Ω and $R_{sh} = 6.644$ Ω. Furthermore, the efficiency of the sample with Ag nanodots is about 14.375% with $V_{oc} = 0.605$ V, $I_{sc} = 7.69$ A and FF = 77.118 with $R_s = 0.00295$ Ω and $R_{sh} = 13.427$ Ω. The low efficiency of the Ref. sample has the very low open circuit voltage. So that no carriers form the photovoltaic circuit due to the formation of short circuit. But the high efficiency of the solar cell printed nano-Ag indicates that printed nano-Ag gets through into PSG layer and forms the Ohmic contact between the n-type Si layer and metal electrode.

The Ref. sample with PSG layer shows a very low efficiency due to the formation of short circuit by the PSG layer. The PSG layer acts as a charge leakage layer between the metal electrodes of screen printed Ag paste and the *n*-type Si emitter layer. After we removed the PSG layer, the cell efficiency of Ref. sample was increased up to 12.72%. For the nano-Ag dots sample with the PSG layer, the cell efficiency of 14.375% indicates that the Ag nanoparticles can prevent the charge leakage from the PSG layer so that the plasmonic effect contributes to the conductive interface for Ohmic contact. To compare to the Ref. sample without the PSG layer, the small enhancement of the cell efficiency of 1.65% may come from the nano-Ag dots contribution of light absorption of surface plasmon. This means that the PSG layer acts as a surface passivation layer where nano-Ag dots can be diffused into the solar cell. Therefore, we conclude that the nano-Ag dots play the roles of both the enhancement of the light conversion efficiency and the formation of surface plasmon.

4. CONCLUSIONS

The nano-Ag dots were patterned on the PSG layer using nano-Ag dots and we deposited SiN_x after nano-Ag printing process. We fabricated the Si solar cell and measured several characteristics. The nano-Ag dots are covered on the SiN_x layer in the standard process, but the nano-Ag dots are located on surface of solar cell from the measurement of FE-SEM images because the SiN_x layer can

be selectively grown up due to the nano-Ag dots. However, the parts without the nano-Ag dots show the normal growth of SiN_x. In the results of measurements of PL and EL, the emission spectra are not much dependent on the densities of the nano-Ag dots, which can decrease the series resistance. Surface plasmonic effect of the nano-Ag dots shows the decrease in photo-reflectance below the wavelength of 376 nm. As the densities of nano-Ag dots are increased, the quantum efficiencies are decreased. The conversion efficiency of Ref. sample with PSG layer is 0.994% due to the PSG layer, and after removing the PSG layer, the cell efficiency of Ref. sample has been increased up to 12.72%. However, the nano-Ag dots sample with the PSG layer shows the cell efficiency of 14.375%. As a concluding remark, the nano-Ag dots play the role of the enhancement of the light conversion efficiency by forming the surface plasmon.

Acknowledgments: This work was supported by the SNT project of the Korea Energy Management Corporation, which is being funded by the Korean government (Grant No. 2008-N-PV12-J-04-1-00).

References and Notes

1. C. Yang, G. Zhang, H. M. Li, and W. J. Yoo, *J. Kor. Phys. Soc.* 56, 1488 (**2010**).
2. J. Choi, B. Parida, J. T. Lee, and K. Kim, *J. Nanosci. Nanotechnol.* 11, 6318 (**2011**).
3. V. E. Ferry, L. A. Sweatlock, D. Pacifici, and H. A. Atwater, *Nano Lett.* 8, 4391 (**2008**).
4. H. S. Chang and H. C. Jung, *J. Nanosci. Nanotechnol.* 11, 3680 (**2011**).
5. T. L. Temple and D. M. Bagnall, *J. Appl. Phys.* 109, 084343 (**2011**).
6. S. Pillai, K. R. Catchpole, T. Trupke, and M. A. Green, *J. Appl. Phys.* 101, 093105 (**2007**).
7. S. H. Lim, W. Mar, P. Matheu, D. Derkacs, and E. T. Yu, *J. Appl. Phys.* 101, 104309 (**2007**).
8. T. L. Temple, G. D. K. Mahanama, H. S. Reehal, and D. M. Bagnall, *Sol. Energy Mater. Sol. Cells* 93, 1978 (**2009**).
9. E. Moulin, J. Sukmanowski, M. Schulte, A. Gordijn, F. X. Royer, and H. Stiebig, *J. Non-Crys. Solids* 354, 2488 (**2008**).
10. D. M. N. M. Dissanayake, B. Roberts, and P. C. Ku, *Appl. Phys. Lett.* 99, 113306 (**2011**).
11. Z. Ouyang, S. Pillai, F. Beck, O. Kunz, S. Varlamov, K. R. Catchpole, P. Campbell, and M. A. Green, *Appl. Phys. Lett.* 96, 261109 (**2010**).
12. K. N. Jeon, S. H. Kim, H. J. Kim, I. S. Kim, and S. H. Kim, *Trans. Electr. Electron. Matter.* 12, 204 (**2011**).
13. J. Heo, *Trans. Electr. Electron. Matter.* 13, 35 (**2012**).
14. Z. H. Li, S. C. Roh, D. Y. Ryu, J. H. Choi, H. I. Seo, and Y. C. Kim, *Trans. Electr. Electron. Matter.* 12, 156 (**2011**).
15. F. J. Beck, A. Polman, and K. R. Catchpole, *J. Appl. Phys.* 105, 114310 (**2009**).
16. G. Xu, M. Tazawa, P. Jin, S. Nakao, and K. Yoshimura, *Appl. Phys. Lett.* 82, 3811 (**2003**).
17. B. P. Salomon, S. Gall, R. Monna, S. Manuel, and A. Slaoui, *Sol. Energy Mater. Sol. Cells* 95, 2536 (**2011**).
18. H. C. Liu, C. P. Chuang, Y. T. Chen, and C. H. Du, *Water Air Soil Pollut.: Focus* 9, 495 (**2009**).
19. L. C. Tien, D. P. Nortion, S. J. Pearton, H. T. Wang, and F. Ren, *Appl. Surf.* 253, 4620 (**2007**).
20. W. I. Park, G. C. Yi, J. W. Kim, and S. M. Park, *Appl. Phys. Lett.* 82, 4358 (**2003**).
21. E. C. Garnett and P. Yang, *J. Am. Chem. Soc.* 130, 9224 (**2008**).
22. Y. A. Akimov, K. Ostrikov, and E. P. Li, *Plasmonics* 4, 107 (**2009**).
23. U. Kreibig and M. Volmer, Optical Properties of Metal Clusters, Springer Series in Materials Science 25, Springer, Heidelberg (**1995**), p. 51.
24. C. Eminian, F. J. Haug, O. Cuberto, X. Niquille, and C. Ballif, *Prog. Photovolt: Res. Appl.* 19, 260 (**2010**).

Received: 1 August 2011. Accepted: 12 January 2012.